Award Number: DAMD17-01-1-0064

TITLE: Endourethral MRI Guidance for Prostatic RF Ablation

PRINCIPAL INVESTIGATOR: Ergin Atalar, Ph.D.

CONTRACTING ORGANIZATION: Johns Hopkins University School of Medicine
Baltimore, Maryland 21205

REPORT DATE: June 2003

TYPE OF REPORT: Annual

PREPARED FOR: U.S. Army Medical Research and Materiel Command
Fort Detrick, Maryland 21702-5012

REPORT DOCUMENTATION PAGE

Form Approved
OMB No. 074-0188

1. AGENCY USE ONLY (Leave blank)	2. REPORT DATE	3. REPORT TYPE AND DATES COVERED
	June 2003	Annual (1 Jun 02 - 31 May 03)

4. TITLE AND SUBTITLE
Endourethral MRI Guidance for Prostatic RF Ablation

5. FUNDING NUMBERS
DAMD17-01-1-0064

6. AUTHOR(S)
Ergin Atalar, Ph.D.

7. PERFORMING ORGANIZATION NAME(S) AND ADDRESS(ES)
Johns Hopkins University School of Medicine
Baltimore, Maryland 21205
E-Mail: eatalar@mri.jhu.edu

8. PERFORMING ORGANIZATION REPORT NUMBER

9. SPONSORING / MONITORING AGENCY NAME(S) AND ADDRESS(ES)
U.S. Army Medical Research and Materiel Command
Fort Detrick, Maryland 21702-5012

10. SPONSORING / MONITORING AGENCY REPORT NUMBER

11. SUPPLEMENTARY NOTES

12a. DISTRIBUTION / AVAILABILITY STATEMENT
Approved for Public Release; Distribution Unlimited

12b. DISTRIBUTION CODE

13. ABSTRACT (Maximum 200 Words)

Prostate cancer constitutes a major health problem. Although the medical techniques currently in use to diagnose prostate cancer are successful, the methods to stage the cancer and visualize the invasion and spread of the cancer are inadequate. MRI is known to be the best method for staging but it does not offer image resolution that is acceptable, especially for detecting disease in the anterior prostate. In the first year of the project, we have developed a phased array coil setup that enabled us imaging of the prostate with 160 microns image resolution. The second year, we have developed a mechanical setup that enabled placement of the needles in the prostate with 1mm accuracy. Both of these are published in high impact journals. Developed methods for imaging temperature changes in the prostate with high accuracy. In the last year of the project, we will test the performance of this setup on animals in precise RF ablation of the prostate.

14. SUBJECT TERMS
MRI, RF ablation of Prostate, MRI-guided interventions

15. NUMBER OF PAGES
43

16. PRICE CODE

17. SECURITY CLASSIFICATION OF REPORT	18. SECURITY CLASSIFICATION OF THIS PAGE	19. SECURITY CLASSIFICATION OF ABSTRACT	20. LIMITATION OF ABSTRACT
Unclassified	Unclassified	Unclassified	Unlimited

Table of Contents

A. Introduction

The specific aims of the project were stated as follows in the original application:

We believe that the success of MR-guided therapy of the prostate depends on the improvement in signal-to-noise ratio. Currently, open MR magnets are used for MR-guided thermal therapy. Unfortunately, studies carried out in open magnets suffer from low SNR because of (a) low main magnetic field (it is known that field strength and SNR have a linear relation) and (b) the coils designed for the open magnets are not optimal because scanner manufacturers do not put enough effort into their development. We, therefore, plan to investigate the use of optimum RF coils in high-field short magnets for real-time monitoring of the RF ablation process. More specifically:

Aim 1. We will develop novel MRI probes for acquisition of ultra-high resolution images of the prostate.

Aim 1a. Based on the single-loop technology developed in our lab, we will design tiny and flexible endo-urethral probes with mechanical properties similar to Foley catheters. To obtain maximum performance, we will combine these probes with a homemade endo-rectal MRI probe and two homemade pelvic coils in a phased array combination.

Aim 1b. We will measure the performance of this design on a phantom and compare the results with the ultimate intrinsic SNR.

Aim 1c. We will test the performance and safety of the phased array coil for high-resolution imaging of the prostate on a dog model.

Aim 2. We will test the hypothesis that RF therapy of the prostate can be monitored using real-time MRI techniques on a dog model. For this purpose:

Aim 2a. We will construct an MR-compatible RFT needle in the form of an MRI antenna and connect it to the phased array coil developed in the previous aim to visualize the position of the needle and surrounding tissue during the ablation procedure.

Aim 2b. We will test the hypothesis that RF ablation of the prostate can be monitored in vivo on a dog model.

Aim 3. We will test the hypothesis that MR-guided RF ablation procedures can be carried out without a significant risk of morbidity and mortality on dogs. We plan to use histology as the gold standard for comparison, from which we will derive an effectiveness versus morbidity curve that could be used by clinicians to help determine the extent of ablation therapy.

Our overall aim is to develop an MR-guided prostate therapy system. After successful completion of this project, we will seek further funding to investigate the use of the developed system on human patients.

As in the previous year, we are slightly ahead of the original timeline in the project. First aim 1 of the project is completed. Second aim is almost complete. We already started the third aim of the project. Our high pace in the project is partly related with the synergetic funds obtained from National Science Foundation, which enabled us to work closely with researchers at the Johns Hopkins Mechanical Engineering Department, Computer Science Department and also at NIH.

B. Body

B.1. *Coil Design.*

In this study, we designed a prostate phased array system that consisted of one 3-inch surface coil (General Electric), one endourethral coil, and two endorectal coils. Two types of endourethral coils were investigated: a loopless design that fit into a 2.5 mm diameter sheath; and a loop design that fit into a 5.3 mm diameter sheath. Two 1.3 x 2 cm rectal loop coils were mounted on the same probe, with the amount of overlap set so that interloop flux was minimized to ensure isolation. All coils were matched and decoupled by the appropriate circuitry. The safety analysis of this design has been completed and tested on animals.

B.2. *Accurate Needle Placement*

A micro coil tracking method has been developed to quickly (50 msec) and accurately (mean micro coil position error < 1 mm) locate the position and orientation of an intrarectal needle guide within the MR imaging volume. Via a mechanical positioning mechanism and extended control rods, the needle guide can be rotated and translated from outside of the closed scanner bore. Once the needle guide is positioned on the proper trajectory, the RF needle can be inserted to a controlled depth via an offset stop. The needle guide was situated inside a stationary rectal sheath that served to minimize prostate motion and also housed a local imaging coil.

We placed gold seeds in a dog prostate using this technique and measured the position of the seeds in order to test the accuracy of the needle positioning mechanism. We also injected blue dye and contrast agent mixture to the prostate with the purpose of developing an accurate prostate treatment technique. This method of MR-guided injection of therapeutic agents attracted attention in the research community. We plan to seek funding in the future to continue in this direction.

As mentioned earlier, achievement of this complex task in a short time was possible because of the synergetic fund from National Science Foundation and collaboration from various researchers at NIH and JHU. We plan to continue collaboration with these researchers in order to keep the high pace of the research in the third year of the project.

C. Key Research Accomplishments

We have completed the first aim of the project and are close to completion of the specific Aim 2 of the project. This is slightly ahead of the original timeline of the project.

D. Reportable Outcomes

Our paper on the phased coil design to Magnetic Resonance in Medicine has been published, which concludes the specific aim 1 of the project. As a part of second aim, the mechanical design of the high-precision placement of the needles in the prostate will be published in Radiology. In addition two these two peer reviewed journals, we have presented four abstracts in the conferences as given in the references.

E. Conclusions

We completed Aim 1 and most of Aim 2 of the study. We have published two peer reviewed journal articles. We plan to complete the second aim and the third aims of the project and publish our results in a peer-reviewed journal in the last year of the project.

F. References

First Year

1. A. C. Yung, Y. A. Oner, J. M. Serfaty, M. Feleney, X. Yang, E. Atalar, Phased Array Coils for High Resolution Prostate MR Imaging, IEEE EMBS, Istanbul, Turkey, 2001.
2. A. .C Yung, A. Y. Oner, J. M. Serfaty, M. Feneley, X. Yang, E. Atalar, High Resolution Imaging of Canine Prostate using Endorectal/Endourethral Phased Array Coils, ISMRM, Book of abstracts Paper#1896, Honolulu, HI, 2002.

Second Year

3. R. C. Susil, A. Krieger, J. A. Derbyshire, L. L. Whitcomb, G. Fichtinger, E. Atalar, "MRI Guided Intraprostatic Therapeutic Injections in a Closed, 1.5T Scanner", Accepted to ISMRM 2003.
4. R. C. Susil, K. Camphausen, E. Atalar, E. R. McVeigh, H. Ning, R. W. Miller, C. N. Coleman, C. Menard *"MRI Guidance and Planning for High-Dose-Rate Brachytherapy (HDRT) of the Prostate"* Accepted to ISMRM 2003.
5. R.C. Susil, A. Krieger, J.A. Derbyshire, A. Tanacs, E.R. McVeigh, L.L. Whitcomb, G. Fichtinger, E. Atalar, *"A System for Guidance and Monitoring of Transrectal Prostate Biopsy in a 1.5 T Closed MR Scanner"*. iMRI Meeting, Leipzig, Germany, published in Eur. Radiology vol: 12, page F3, 2002.
6. V. C. Shah, A. El-Sharkawy, X. Du, X. Yang, E. Atalar, "MR signal for one pixel Temperature in °C SSFP based MR Thermometry", Accepted to ISMRM 2003.
7. R. C. Susil, A. Krieger, J. A. Derbyshire, A. Tanacs, L. L. Whitcomb, G. Fichtinger, E. Atalar, A System for MRI Guided Prostate Interventions, Radiology, Accepted, 2002.
8. A. Yung, Y. Oner, J. M. Serfaty, M. Feleney, X. Yang, E. Atalar, Phased array MRI of canine prostate using endorectal and endourethral coils, Magnetic Resonance in Medicine, 49(4) 710-715, 2003.

A System for MRI Guided Prostate Interventions – A Canine Study

Robert C. Susil[1] BS, Axel Krieger[2] MS, J. Andrew Derbyshire[3] PhD, Attila Tanacs[4] BS, Louis L. Whitcomb[2] PhD, Gabor Fichtinger[4] PhD, Ergin Atalar[5,6*] PhD

Johns Hopkins University [1]Department of Biomedical Engineering, [2]Mechanical Engineering, [4]Computer Science, and [5]Radiology
Baltimore, Maryland

[3]Laboratory of Cardiac Energetics, National Institutes of Health
Bethesda, Maryland

[6]Department of Electrical Engineering, Bilkent University
Ankara, Turkey

Radiology, In Press

*Correspondence and Originating Institution:
Ergin Atalar, Ph.D.
Johns Hopkins University Department of Radiology
Johns Hopkins Outpatient Center Room 4241
601 N. Caroline St.
Baltimore, MD 21287-0845
Phone: (410) 955-9617
FAX: (410) 614-1977
e-mail: eatalar@mri.jhu.edu

Grant Support: Supported in part by NIH grants R01 HL57483 and R01 HL61672. Additional support from NSF grant ERC 9731478 and US Army grant PC 10029. RCS is supported by an NIH training grant.

Submission Type: Original Research

ABSTRACT

PURPOSE: A transrectal system allowing for precise, image guided and monitored prostate interventions within a 1.5T MRI scanner is demonstrated.

METHODS: Using a microcoil tracking method, a remotely-actuated intrarectal needle guide, and an intrarectal sheath including a local imaging coil, the system is applied for MRI monitored intraprostatic injections and brachytherapy seed placement. Importantly, it is useable within a closed, 1.5 T scanner and therefore, can capitalize on the higher SNR provided by traditional magnet designs, which is crucial for accurate targeting and monitoring of prostate interventions. In four canine studies, the functionality and applications of this system are shown.

RESULTS: In the first canine, reliable needle placement, with an accuracy of approximately 2 mm, is demonstrated. In two therapeutic demonstrations, MR imaging is used to monitor the distribution of an injected agent in and around the prostate (here, Gd-DTPA mixed with Trypan blue tissue dye), confirming that the drug has covered the desired tissue and also detecting faulty injections. In a final therapeutic example, accurate placement and MR visualization of brachytherapy seeds within the prostate is demonstrated.

CONCLUSION: The system provides a flexible platform for a variety of minimally invasive, MRI-guided therapeutic and diagnostic prostate interventions.

KEYWORDS: Prostate, MR; Prostate neoplasms, MR; Prostate neoplasms, therapy; Prostate neoplasms, therapeutic radiology; Magnetic resonance (MR), guidance; Magnetic resonance (MR), experimental studies

INTRODUCTION

Prostate carcinoma is the most commonly diagnosed serious cancer in US males with a projected annual incidence of 189,000 for 2002 (1). As incidence is known to increase with age, prevalence of this cancer will likely continue to increase as the US population ages (2). Moreover, due to the widespread acceptance of PSA screening, routine rectal examination, and transrectal US guided prostate biopsy, there has been a great increase in early detection of prostate cancer (3).

Despite this, the proper clinical management of prostate cancer is very controversial. Serious debate exists as to the clinical relevance of low-grade prostate cancer. In some cases, prostate cancer will grow very slowly and never become clinically significant while in other cases, it can be very aggressive and dangerous. As more than 30% percent of men over 50 have incidentally discovered focuses of prostate cancer on autopsy (unrelated to the actual cause of death), its clear that aggressive treatment is not always appropriate for this cancer (4,5). Nevertheless, recent reports have shown that overly conservative management (i.e. 'watchful waiting') can produce poor outcomes (6-8). Clinical decision making is further complicated by the fact that most prostate cancers are assessed as 'intermediate stage' and therefore carry an uncertain prognosis (9).

Currently, the two most accepted treatment methods for localized prostate cancer are radical prostatectomy and radiation therapy (10). While both of these approaches offer a good chance of cure, they also carry significant chance of morbidity including incontinence, rectal toxicity, and erectile dysfunction (11). Given this, efforts have increased toward developing focal, minimally invasive treatment modalities that can target cancerous tissue while reducing morbidity and treatment duration (12).

Effective image guidance for these minimally-invasive therapies requires (1) excellent visualization of the prostate and surrounding anatomy, such that cancerous tissue can be treated while avoiding nearby neural and vascular structures, and (2) visualization of the therapeutic agent itself, such that there is direct confirmation that the desired abnormal tissue has been treated. Based on these conditions, Magnetic Resonance Imaging is the best choice for image-guidance because of its high resolution, excellent soft tissue contrast, multiplanar capabilities, and the potential to yield spectral/biological information (13). MRI has been shown to deliver far better visualization of the prostate and surrounding structures than either ultrasound or CT (14). Moreover, with MRI it is possible to visualize injected liquids agents (15,16); solid, implanted therapeutic seeds (e.g. brachytherapy seeds) (14,17); and thermal therapy (through both direct temperature monitoring and imaging of tissue damage) (18,19). We emphasize that the ability to visualize the therapeutic agent itself is very enabling in that it allows for direct, positive confirmation of treatment delivery.

In this work, we describe a system that allows for precise, monitored prostate therapy delivery inside of a 1.5 T MRI scanner. This system uses a standard, transrectal approach to the prostate as opposed to access through the perineum (20). Also, the system does not require an open scanner architecture and therefore, can capitalize on the higher SNR provided by traditional magnet designs, which is crucial for accurate targeting and therapy monitoring (14).

In a canine model, we show that needles can be reliably placed in the body of the prostate with an accuracy of <2 mm. Then, in a therapeutic demonstration, we show that MR imaging can be used to monitor the distribution of an injected agent (here, Gd-DTPA

mixed with Trypan blue tissue dye), confirming that the drug has covered the desired tissue and also detecting faulty injections. In a second therapeutic example, we show that brachytherapy seeds can be accurately placed and visualized within the prostate using MR guidance.

METHODS

A mechanically actuated, transrectal needle guide is used to perform MR guided needle placements in the prostate. With a microcoil tracking method, we are able to quickly and accurately locate the position and orientation of the needle guide in the MR imaging volume (60 msec). Knowing the position of the needle allows for acquisition of realtime images of a plane including the needle and registration of the needle position with previously acquired, high-resolution images of the prostate. In four canine studies, we demonstrate the functionality and applications of this system.

DEVICE DESIGN

A thin-walled, cylindrical plastic sheath (Delrin plastic, DuPont Inc., Wilmington, Delaware) with a radius of 1.5 cm is inserted into the subject's rectum, forming a stable and stationary entry point through which the prostate can be accessed (Figure 1a). Integral to the sheath is a single turn imaging loop (with a diameter of 2.5 cm) for local imaging of the prostate. The sheath has a window, located within the imaging loop, such that a needle can be advanced from inside the sheath, through the rectal wall, and into the body of the prostate.

Next, a cylindrical needle guide (Figure 1b), also made of Delrin plastic, is placed within the rectal sheath (Figure 1c). As the needle guide is coaxial with the rectal sheath, the needle guide is free to rotate and translate within the cavity formed by the sheath without causing deformation of the surrounding soft tissue. Integral to the needle guide are (1) three microcoil fiducials and (2) a curved channel for the needle (Figure 1D). Note that because the needle channel is curved, the needle can be inserted along the axis of the needle guide and emerge out of its lateral wall, allowing for access to the prostate through the window in the stationary rectal sheath.

Next, both the rectal sheath and the needle guide are affixed to a positioning stage (Figure 2a) made of Nylon plastic (QTC, New Hyde Park, New York) and Delrin. First, this positioning stage serves to hold the rectal sheath stationary within the subject's rectum. A linear track (aluminum rail, 80/20 Inc., Columbia City, Indiana) and a polyamide plastic articulated-arm with six joints allow for full mobility of the positioning stage, such that it can be easily docked with the rectal sheath (Figure 2b), at which point the linear track and articulated arm are locked down to prevent any subsequent motion.

In addition to holding the rectal sheath stationary, the positioning stage contains a screw drive mechanism that allows for both rotation and translation of the needle guide. This device converts rotation of two concentric control rods (Epoxy tubing, TAP Plastics, Dublin, California), both of which extend outside of the scanner bore, into rotation and translation of the needle guide – allowing the operator to position the needle guide while the subject is within the closed bore scanner (Figure 2c).

As the entire device is constructed with a coaxial design, the central axis offers an unobstructed path for insertion of the needle. The depth of needle insertion is controlled

using a variable offset stop that is inserted at the back of the device before introducing the needle (Figure 3a). An 18G coaxial needle (MRI Devices Daum GmbH, Schwerin, Germany) is inserted such that the needle tip emerges from the side of the needle guide.

DEVICE TRACKING, PROSTATE TARGETING, AND REALTIME IMAGING

MR pulse sequences and hardware were designed to facilitate targeted needle placement in the prostate within a GE 1.5 T CV/i MRI scanner with 4 independent receiver channels. Three microcoil fiducials were integrated within a transrectal needle guide (Figure 1d), each connected to a separate receiver channel. To determine the position and orientation of these coils, twelve 1-D dodecahedrally spaced readouts were collected (TE 2.3 msec, TR 5.0 msec, BW +/-64 KHz, FA 1^{o}, FOV 40cm, 256 readout points), allowing for coil localization, as described previously (21,22). The coil localization scan occupied ~ 60 msec. Microcoil location errors due to gradient nonlinearity were removed using gradient dewarping algorithms (GE Medical Systems, Waukesha, Wisconsin).

Given the position of the three microcoil fiducials in the MR coordinate system and the location of a given intraprostatic target (also in the MR coordinate system), the remaining problem is to determine (1) the rotation and translation necessary to position the needle guide such that the needle trajectory is aligned with the target and (2) the amount of needle insertion necessary to reach the target. This can be calculated using a set of coordinate transformations - assuming that the relationship between the microcoil positions, the device axis, and the needle trajectory are all known. These relationships are established using a device calibration scan in which Gd-DTPA (Magnevist, Berlex Laboratories, Wayne, New Jersey) fiducial tubes define the device axis and the needle

trajectory (the same, single calibration scan was used for all studies described here). In addition to determining the rotation and translation necessary to reach the target site, the calibration of the microcoil positions with the needle trajectory allowed for definition of a scan plane that includes both the needle path and the device axis. 'Realtime' images were acquired based on the current position of the microcoil fiducials, such that the needle could be visualized as it was inserted into the prostate.

All experiments were performed on a GE 1.5 T CV/I MRI scanner (GE Medical Systems, Waukesha, Wisconsin). A fast gradient-echo pulse sequence (FGRE) was modified to allow for alternating acquisition of the microcoil-tracking readouts (i.e. the twelve, dodecahedrally spaced readouts) and realtime FGRE images. After the location of each coil was determined, the position and orientation of the imaging plane is defined such that the realtime FGRE image slice tracked with the position of the needle.

Realtime data processing and display were performed using a Sun Ultra II Workstation (Sun Microsystems, Mountain View, California) connected to the scanner with a high-bandwidth data bus (SBS Technologies, Carlsbad, California). In the current implementation, the tracking sequence takes 60 msec; image processing, communication, and scan plane localization occupies 150 msec; and imaging takes 300 to 1300 msec – yielding frame rates of 0.7 to 2 fps (depending predominantly on image acquisition time). Images were acquired using rectal imaging coil while the other three receiver channels were used for the microcoil fiducials.

ANIMAL PROTOCOL

All animal protocols were reviewed and approved by the insititution's Animal Care and Use Committee. Four mongrel dogs weighing approximately 25 kg were

anesthetized with a bolus injection of thiopental and maintained on 1% isoflurane throughout the experiment. An intravenous catheter was placed in the right jugular vein for fluid administration and a Foley catheter was inserted to aid in stabilizing the prostate and to define the position of the prostatic urethra. The animals were placed prone on the scanner table with the pelvis slightly elevated (~ 10 cm) with a 5-inch surface coil on the anterior surface of the abdomen at the level of the prostate. The rectal sheath was inserted into the rectum and docked with the positioning stage, which was then locked in place (Figure 2b).

NEEDLE PLACEMENT PROTOCOL

In the first animal study, the accuracy of needle placement was tested in-vivo. After the animal was positioned in the scanner, T1 weighted FSE images of the prostate and surrounding anatomy were acquired (TE 9.2 msec, TR 700 msec, BW +/-31.25 KHz, ETL 4, FOV 16cm, slice thickness 3mm, interslice spacing 0.5mm, 256x256, NEX=4, scan time 3:00). Two receiver channels were used for these images: one for the 5-inch surface coil and one for the rectal coil. In these images, a target was selected within the body of the prostate and entered into the realtime control program. Scanning was then switched to the realtime FGRE imaging and tracking sequence.

While running the realtime FGRE imaging and tracking sequence, the operator is able to rotate and translate the needle guide from outside of the scanner bore by rotating the two, coaxial control rods (Figure 2c). On a scan room flat panel display, the operator watches both the realtime image slice, showing the trajectory of the needle, as well numerical values indicating the current amount of rotation and translation necessary to set

the correct needle trajectory. As the needle guide is moved closer to the target position, these numbers move to zero – indicating that no more rotation or translation is necessary.

Once the needle guide on the proper trajectory, the insertion stop is set to the proper depth (also indicated on the flat panel display) and the needle is pushed until it is flush with the stop (Figure 3a). The insertion of the needle can be visualized on the scan room display and once in place, the needle tip will be at the desired target location.

To confirm the location of the needle tip, a second set of T1 weighted FSE images were acquired. This protocol was repeated for four separate needle insertions.

INTRAPROSTATIC INJECTION PROTOCOL

To demonstrate MR monitored injection therapies, intraprostatic injections were preformed in two canine subjects. Similar to the needle placement protocol, targets in the prostate were selected on axial T1 weighted FSE images and the needle tip was placed at these locations using the realtime FGRE imaging and tracking sequence. After the coaxial needle was placed, the trocar (i.e. an inner stylus) was withdrawn, leaving only the 18G cannula (i.e. a hollow metal tube) in place. This provided a conduit through which injections into the body of the prostate could be performed (Figure 3b). In this demonstration, a mixture of 0.4% Trypan Blue (Sigma-Aldrich, St. Louis, Missouri) and 30 mM Gd-DTPA (Magnevist, Berlex Laboratories, Wayne, New Jersey) was injected. 0.3 mL of this solution was injected into the prostate. During the injection, the flow of the mixture was monitored using a high flip-angle, RF-spoiled, gradient echo imaging sequence (FSPGR, TE 1.5 msec, TR 6 msec, FA 90^{o}, BW +/-62.5KHz, FOV 16cm, slice thickness 10mm, 256x160, 0.96 sec/image). The location of the injected solution was determined by comparing gradient echo axial images acquired both before and after the

injection (FSPGR, TE 2.0 msec, TR 80 msec, FA 60°, BW +/-31.25KHz, FOV 16cm, slice thickness 3mm, interslice spacing 0.5mm, 256x256, NEX 4, scan time 1:20).

BRACHYTHERAPY SEED PLACEMENT PROTOCOL

In a fourth canine, the use of this device for MR guided brachytherapy seed placement was demonstrated. Targets were selected and the trocar and canula were placed (Figure 3c), as described previously. Then, to insert the titanium brachytherapy seeds (OncoSeed blanks, Medi-Physics Inc., Arlington Heights, Illinois), the trocar was withdrawn, leaving the hollow cannula in place within the prostate. A brachytherapy seed was inserted into the cannula and then advanced to the end, but not out, of the cannula by pushing it with another trocar (Figure 3d). With the seed at the end of the cannula, the cannula was withdrawn slightly while holding the trocar stationary, causing the brachytherapy seed to be ejected into the prostate tissue. Subsequently, the trocar and cannula were both withdrawn together (Figure 3e). Three seeds were placed using this technique. The location of the needle and of the seeds was confirmed using T1 weighted FSE images (TE 9.2 msec, TR 700 msec, BW +/-31.25 KHz, ETL 4, FOV 16cm, slice thickness 3mm, interslice spacing 0.5mm, 256x256, NEX=4, scan time 3:00).

RESULTS

MR GUIDANCE ALLOWS FOR NEEDLE PLACEMENT WITHIN THE PROSTATE GLAND WITH MILLIMETER ACCURACY

In the first canine subject, accurate needle placement within the body of the prostate is demonstrated. The results of this study are summarized in Figure 4. In

sequential order, four targets were selected from T1 weighted FSE images (Figure 4, top row). Having placed the needle using the FGRE realtime imaging and tracking sequence, FSE images were repeated to confirm placement of the needle by visualizing the needle void (Figure 4, bottom row). In all cases, the end of the needle artifact was found in the same image slice as the target (slice thickness = 3mm). Moreover, the center of the needle tip void was found within 2 mm (in-plane) of the selected target. Note also that there is minimal motion of the prostate upon insertion of the needle.

For interpretation of these results, it is necessary to examine the artifact created by the 18G MR compatible needle. Figure 5 shows the artifact created both by the needle and by a brachytherapy seed. Artifacts were aligned by placing the physical objects at the interface of gadolinium doped and gadolinium free gel blocks. Note that the tip void is a circular bloom that is centered on the physical end of the needle, as has been previously reported when the needle is aligned approximately parallel to B_0 with the tip toward the positive magnet pole (23). In all cases, because of the design of the needle placement system, the needle is approximately parallel to B_0 and therefore, the artifact provides a good estimate of the needle tip position.

In phantom trials that allow for direct, visual confirmation of needle placement accuracy, the needle tip consistently hit spherical targets with a radius of 2 mm (results not shown). Because visual confirmation is not possible in vivo, it is difficult to precisely quantify the in vivo needle placement accuracy. However, in all in vivo experiments, the needle tip was within the same slice as the target (slice thickness = 3mm), and the in-plane needle position error was less than 2 mm. Therefore, the phantom and in vivo results appear to be consistent.

INTRAPROSTATIC INJECTIONS CAN BE VISUALIZED AND MONITORED USING MRI

In two canine subjects, the use of the system for MR monitored intraprostatic injections was demonstrated. First, a target within the body of the prostate gland was selected and the needle was positioned as described in the previous section. Then, the trocar was withdrawn, leaving the cannula as a conduit into the prostate. A mixture of 30 mM Gd-DTPA and 0.4% Trypan Blue (16) was then injected into the prostate. A high flip-angle, RF-spoiled, gradient echo acquisition was run during the injection of 0.3 mL of this solution. The box on the sagittal scout (Figure 6, left image) shows the location of the time series images. Note that all of the injected contrast/dye solution stays confined within the prostate. Therefore, it was confirmed – during the injection - that the full, desired dose was delivered to the prostate tissue.

In Figure 7, the distribution of the mixture as shown in the MR images is compared with that revealed on histology. There is good correlation between the tissue enhancement (seen in the second column, after the injection, but not in the first column, before the injection) and the tissue stained with the Trypan Blue dye (Figure 7, third column).

In the next canine, the injection protocol was repeated as before. In this case, however, the injected contrast/dye solution is seen to leak out of the prostate and into the surrounding connective tissue (Figure 8). Therefore, it is known – *during the procedure* – that the desired dose has not been delivered to the prostate. In Figure 9, the presence of Trypan Blue in connective tissue at the superior margin of the prostate is confirmed histologically.

BRACHYTHERAPY SEED PLACEMENT CAN BE PLANNED AND VERIFIED USING MRI

In the last canine subject, the application of the system for placing brachytherapy seeds within the prostate is demonstrated. The results of this study – in which three seeds were placed in the prostate – are summarized in Figure 10. As described previously, three targets were selected, in succession, within the body of the prostate (Figure 10, row a) and the needle was placed using the realtime FGRE imaging and tracking sequence (Figure 10, row b). As compared with the needle placement study (Figure 4), the tip of the needle artifact is seen to extend beyond the target point. This is because the brachytherapy seeds are placed at the end of the cannula, *not* at the end of the trocar. As seen in Figure 3c, the trocar extends 2 mm past the end of the cannula. Therefore, for proper seed deposition, the trocar must extend 2 mm past the target point, as seen in Figure 10, row b.

In Figure 10, row c, the seeds are placed in the prostate and the coaxial needle has been removed. To interpret these results, refer to Figure 5, where the artifact pattern for the brachytherapy seeds is displayed. The main signal void is found at the *end* of the 4 mm seed that lies nearest to the positive pole of B_0. This corresponds to the black void seen in Figure 10, row c. The bodies of the brachytherapy seeds extend 4 mm in the inferior direction from this void (in the direction of the target location). The seeds lie within 3 mm of the selected target location. Also, note that intraprostatic bleeding, resulting from seed placement, can be seen near seeds 2 and 3 (i.e. the dark banding radiating toward the edge of the prostate).

DISCUSSION

MR GUIDED PROSTATE BIOPSY MAY FACILITATE IMPROVED TUMOR MONITORING AND DIAGNOSIS

We have shown that needles can be accurately placed in the body of the prostate gland while the subject is within a closed bore, 1.5 T MR scanner. While diagnostic biopsy was not a focus of the current study, it is an obvious subsequent application. Currently, transrectal ultrasound (TRUS) guided needle biopsy is the gold standard for the diagnosis of prostate cancer (24). Although this method has excellent specificity, it is not very sensitive. TRUS-guided biopsy fails to correctly detect the presence of prostate cancer in approximately 20% of cases (25). MRI, in contrast, has a high sensitivity for detecting prostate tumors (26). Unfortunately, MR imaging alone, without concurrent biopsy, suffers from low diagnostic specificity. Therefore, to take advantage of the high diagnostic sensitivity of MRI while maintaining the specificity of biopsy, this system may be ideal for performing MRI guided prostate biopsy. While it would not be practical to perform all prostate biopsy under MR guidance, the excellent tissue contrast provided by MR is very useful for targeted tissue biopsy. In cases where men have consistently rising PSA levels (indicating a high likelihood of cancer) but repeated negative ultrasound guided biopsies, MR image guided biopsy may provide a definitive diagnosis. The utility of MRI in this application area has been demonstrated in a low-field, open magnet using a transperineal approach to the prostate (20). The present system is ideal for this application is that it uses the standard, transrectal approach to the prostate and is useable within closed bore scanners, providing higher SNR vital for tumor visualization.

Second, MRI targeted prostate biopsy may provide the level of anatomical accuracy that is necessary for chronic monitoring of prostate lesions. With current ultrasound guided biopsy, it is very difficult to repeatedly collect tissue from the same location within the prostate because of poor anatomical visualization. Given the current rise in early detection of prostate cancers and the prevalence of medium stage tumors, which carry an uncertain prognosis (9), it would be very useful to be able to repeatedly 'sample' a tumor over a matter of years. This would allow for better clinical decision making, delaying definitive prostatectomy or radiation therapy until absolutely necessary (and possibly indefinitely).

MR VISUALIZATION OF INTRAPROSTATIC INJECTIONS ALLOWS FOR VERIFICATION OF TREATMENT DELIVERY AND DETECTION OF FAULTY INJECTIONS

Using MRI, the distribution of therapeutic agents, injected into the prostate, can be directly verified with high spatial resolution. MRI provides not only excellent visualization of the tissue itself, but also of the therapeutic agent. It is therefore easy to verify when the desired tissue has been treated and also, most importantly, when an injection has failed, sending the injected substance into surrounding tissue rather than into the desired target area. With the advent of local, targeted treatments for prostate cancer (12,27), it is vital to confirm that therapy placement has been successful. Otherwise, potentially valuable agents could be labeled as being ineffective simply because the therapy never reaches the target site.

MRI ALLOWS FOR IMPROVED PLANNING AND ASSEMENT OF BRACHYTHERAPY SEED PLACEMENT

In the final study of this work, the utility of MRI for guiding brachytherapy seed placement was demonstrated. Commonly, brachytherapy seeds are placed using transrectal ultrasound guidance while the seeds are inserted through the perineal surface (28). Given the poor soft tissue contrast provided by ultrasound, however, it is common for the seeds to become misplaced into nearby tissue (29). In a recent study, radiation seeds were found in the lungs of 36% of patients after ultrasound guided prostate brachytherapy (seeds may be inadvertently placed in the venous plexus surrounding the prostate, where they can then travel to the lungs) (30). In these cases, MR guided seed placement, showing good anatomical definition, has clear utility. This type of system would be best suited for the placement of a few therapy seeds near a small lesion in the prostate.

KEY SYSTEM COMPONENTS

Two important aspects of the current system design are emphasized. First, the stationary rectal sheath is essential for both high-resolution imaging and stability of the prostate. The thin walled sheath maintains access to the prostate, providing for easy rotation and translation of the needle guide while minimizing motion of surrounding tissue. As the rectum is very sensitive to pain due to pressure but relatively insensitive to sharp pain, this system will minimize patient discomfort during positioning of the needle guide. Also, the prostate, which is highly deformable, stays relatively fixed throughout the entire procedure (Figures 4 and 10). Without the stationary sheath, motion of the

needle guide would result in significant deformation of the prostate, complicating the targeting procedure.

Second, we emphasize the importance of using the system within a closed, 1.5 T scanner. The main utility of MRI is its high spatial resolution and excellent soft tissue contrast. While a low field, open scanner would simplify the design of the needle guide system, low field strength marginalizes the utility of using MRI in the first place. Therefore, a system was designed that is applicable in a traditional, closed bore magnet such that high quality imaging of the prostate can be maintained.

CONCLUSION

A transrectal system allowing for image monitoring of prostate therapy in a closed, 1.5T MR scanner is described; applications including high resolution monitoring of intraprostatic injections and brachytherapy seed placement are demonstrated. The system employs (1) a microcoil tracking method, (2) a remotely actuated, intrarectal needle guide, and (3) an intrarectal sheath incorporating a local imaging coil. As the system is usable in closed MRI scanners, it can capitalize on the higher SNR provided by traditional magnet designs. The system provides a platform for numerous minimally invasive, image-monitored therapies to treat prostate cancer. Presently, we are investigating injected therapies such as alcohol, chemotherapeutic agents, and genetic agents. This system can also serve as a platform for prostate biopsy, brachytherapy, and tissue ablation (e.g., RF, cryo, or laser).

ACKNOWLEDGMENTS

The authors thank Andrew C H Yung for help with experiments and intrarectal imaging coil design, Jason A Polzin for assistance with gradient dewarping algorithms, Theodore L Deweese for advice on clinical applications, and Elliot R McVeigh for providing additional laboratory and scanner resources.

REFERENCES

1. Jemal A, Thomas A, Murray T, Thun M. Cancer statistics, 2002. CA Cancer J Clin 2002;52(1):23-47.
2. Carter HB, Piantadosi S, Isaacs JT. Clinical evidence for and implications of the multistep development of prostate cancer. J Urol 1990;143(4):742-6.
3. Slawin KM, Ohori M, Dillioglugil O, Scardino PT. Screening for prostate cancer: an analysis of the early experience. CA Cancer J Clin 1995;45(3):134-47.
4. Franks LM. Latent carcinoma of the prostate. J Path Bact 1954;68:603-616.
5. Dhom G. Epidemiologic aspects of latent and clinically manifest carcinoma of the prostate. J Cancer Res Clin Oncol 1983;106(3):210-8.
6. Brasso K, Friis S, Juel K, Jorgensen T, Iversen P. The need for hospital care of patients with clinically localized prostate cancer managed by noncurative intent: a population based registry study. J Urol 2000;163(4):1150-4.
7. Adolfsson J, Steineck G, Hedlund PO. Deferred treatment of clinically localized low-grade prostate cancer: actual 10-year and projected 15-year follow-up of the Karolinska series. Urology 1997;50(5):722-6.
8. Chodak GW, Thisted RA, Gerber GS, Johansson JE, Adolfsson J, Jones GW, Chisholm GD, Moskovitz B, Livne PM, Warner J. Results of conservative management of clinically localized prostate cancer. N Engl J Med 1994;330(4):242-8.

9. Ohori M, Wheeler TM, Scardino PT. The New American Joint Committee on Cancer and International Union Against Cancer TNM classification of prostate cancer. Clinicopathologic correlations. Cancer 1994;74(1):104-14.

10. Pirtskhalaishvili G, Hrebinko RL, Nelson JB. The treatment of prostate cancer: an overview of current options. Cancer Pract 2001;9(6):295-306.

11. Potosky AL, Legler J, Albertsen PC, Stanford JL, Gilliland FD, Hamilton AS, Eley JW, Stephenson RA, Harlan LC. Health outcomes after prostatectomy or radiotherapy for prostate cancer: results from the Prostate Cancer Outcomes Study. J Natl Cancer Inst 2000;92(19):1582-92.

12. Carroll PR, Presti JC, Jr., Small E, Roach M, 3rd. Focal therapy for prostate cancer 1996: maximizing outcome. Urology 1997;49(3A Suppl):84-94.

13. Koutcher JA, Zakian K, Hricak H. Magnetic resonance spectroscopic studies of the prostate. Mol Urol 2000;4(3):143-52;discussion 153.

14. Yu KK, Hricak H. Imaging prostate cancer. Radiol Clin North Am 2000;38(1):59-85, viii.

15. Lederman RJ, Guttman MA, Peters DC, Thompson RB, Sorger JM, Dick AJ, Raman VK, McVeigh ER. Catheter-based endomyocardial injection with real-time magnetic resonance imaging. Circulation 2002;105(11):1282-4.

16. Yang X, Atalar E, Li D, Serfaty JM, Wang D, Kumar A, Cheng L. Magnetic resonance imaging permits in vivo monitoring of catheter-based vascular gene delivery. Circulation 2001;104(14):1588-90.

17. D'Amico AV, Cormack R, Tempany CM, Kumar S, Topulos G, Kooy HM, Coleman CN. Real-time magnetic resonance image-guided interstitial

brachytherapy in the treatment of select patients with clinically localized prostate cancer. Int J Radiat Oncol Biol Phys 1998;42(3):507-15.

18. Chen JC, Moriarty JA, Derbyshire JA, Peters RD, Trachtenberg J, Bell SD, Doyle J, Arrelano R, Wright GA, Henkelman RM and others. Prostate cancer: MR imaging and thermometry during microwave thermal ablation-initial experience. Radiology 2000;214(1):290-7.

19. Graham SJ, Stanisz GJ, Kecojevic A, Bronskill MJ, Henkelman RM. Analysis of changes in MR properties of tissues after heat treatment. Magn Reson Med 1999;42(6):1061-71.

20. Hata N, Jinzaki M, Kacher D, Cormak R, Gering D, Nabavi A, Silverman SG, D'Amico AV, Kikinis R, Jolesz FA and others. MR imaging-guided prostate biopsy with surgical navigation software: device validation and feasibility. Radiology 2001;220(1):263-8.

21. Dumoulin CL, Souza SP, Darrow RD. Real-time position monitoring of invasive devices using magnetic resonance. Magn Reson Med 1993;29(3):411-5.

22. Derbyshire JA, Wright GA, Henkelman RM, Hinks RS. Dynamic scan-plane tracking using MR position monitoring. J Magn Reson Imaging 1998;8(4):924-32.

23. Liu H, Martin AJ, Truwit CL. Interventional MRI at high-field (1.5 T): needle artifacts. J Magn Reson Imaging 1998;8(1):214-9.

24. Presti JC, Jr. Prostate cancer: assessment of risk using digital rectal examination, tumor grade, prostate-specific antigen, and systematic biopsy. Radiol Clin North Am 2000;38(1):49-58.

25. Keetch DW, Catalona WJ, Smith DS. Serial prostatic biopsies in men with persistently elevated serum prostate specific antigen values. J Urol 1994;151(6):1571-4.

26. Wefer AE, Hricak H, Vigneron DB, Coakley FV, Lu Y, Wefer J, Mueller-Lisse U, Carroll PR, Kurhanewicz J. Sextant localization of prostate cancer: comparison of sextant biopsy, magnetic resonance imaging and magnetic resonance spectroscopic imaging with step section histology. J Urol 2000;164(2):400-4.

27. DeWeese TL, van der Poel H, Li S, Mikhak B, Drew R, Goemann M, Hamper U, DeJong R, Detorie N, Rodriguez R and others. A phase I trial of CV706, a replication-competent, PSA selective oncolytic adenovirus, for the treatment of locally recurrent prostate cancer following radiation therapy. Cancer Res 2001;61(20):7464-72.

28. Ragde H, Grado GL, Nadir B, Elgamal AA. Modern prostate brachytherapy. CA Cancer J Clin 2000;50(6):380-93.

29. Coakley FV, Hricak H. Radiologic anatomy of the prostate gland: a clinical approach. Radiol Clin North Am 2000;38(1):15-30.

30. Ankem MK, DeCarvalho VS, Harangozo AM, Hartanto VH, Perrotti M, Han K, Shih WJ, Malka E, White EC, Maggio R and others. Implications of radioactive seed migration to the lungs after prostate brachytherapy. Urology 2002;59(4):555-9.

FIGURE CAPTIONS

Figure 1: Rectal sheath and needle guide. A stationary rectal sheath, with a radius of 1.5 cm, forms a stable access route through which the prostate can be reached (**Panel a**). A single turn rectal imaging coil, with tuning, matching, and decoupling elements, is included in the sheath. A cylindrical needle guide (**Panel b**) is placed inside of the stationary rectal sheath (**Panel c**), allowing for rotational and translational degrees of freedom. The needle guide includes three tracking microcoils and a curved needle channel, allowing for access to the prostate laterally through the wall of the rectum (**Panel d**).

Figure 2: Assembled interventional device. The stationary rectal sheath and needle guide are affixed to the positioning stage (**Panel a**). Via a flexible, articulated arm and a linear track, the device can be positioned freely until both the arm and track are locked into position. The positioning mechanism converts rotation of the two, concentric control rods into rotation and translation of the needle guide within the stationary rectal sheath. The sheath is positioned inside of the subject's rectum and held stationary by the positioning arm and rail (**Panel b**). Via rotation of the two control rods located outside of the bore, the needle guide can be positioned within the rectum (**Panel c**).

Figure 3: Needle insertion and therapy delivery. A variable stop is used to control the insertion depth of the needle (**Panel a**). After removing the trocar (i.e. the inner stylus), the canula remains as a hollow conduit through which fluid can be injected into the

prostate (**Panel b**). To place brachytherapy seeds, the trocar and canula are first advanced together (**Panel c**). Then, after withdrawing the trocar, a brachytherapy seed is pushed to the end of the canula with a second trocar (**Panel d**). Holding the trocar stationary, the canula is withdrawn, ejecting the seed into the tissue (**Panel e**). The trocar and canula are then withdrawn together.

Figure 4: Using the transrectal needle guide and microcoil tracking, needles can be accurately placed within the prostate. In an anesthetized canine, four targets were selected from T1 weighted FSE images (**top row**) (TE 9.2 msec, TR 700 msec, BW +/- 31.25 KHz, ETL 4, FOV 16cm, slice thickness 3mm, interslice spacing 0.5mm, 256x256, NEX=4, scan time 3:00). FSE images were repeated after needle placement (**bottom row**). The needle tip artifact is found in the same slice as the target with an in-plane separation of less than 2 mm. Note also that there is minimal motion of the prostate upon insertion of the needle.

Figure 5: Artifacts created by prostate needle (**Panel a**) and brachytherapy seed (**Panel b**) (FSE, TE 9.2 msec, TR 700 msec, BW +/-31.25KHz, ETL 4, FOV 8 cm, slice thickness 1.5 mm, 256x256, NEX=4, scan time 3:00). Both objects create a uniform signal void along their length and a circular bloom, centered on the object tip, at the end facing the positive pole of the main field. Artifacts were aligned by placing the physical objects at the interface of gadolinium doped and gadolinium free gel blocks.

Figure 6: Intraprostatic injections (here, a solution of 0.4% Trypan Blue and 30 mM Gd-DTPA) can be visualized under MRI. The white box on the sagittal scout (left image) shows the location of the time series images. Note that all of the injected contrast/dye solution stays confined within the prostate. Therefore, it was confirmed that the full, desired dose was delivered to the tissue. (FSPGR, TE 1.5 msec, TR 6 msec, FA 90°, BW +/-62.5KHz, FOV 16cm, slice thickness 10mm, 256x160, 0.96 sec/image).

Figure 7: The distribution of injected material visualized in MR images reflects the actual, histologically confirmed distribution. Gadolinium-DTPA location (enhancement seen in post- but not pre-injection images) matches with blue stained tissue in the canine prostate (FSPGR, TE 2.0 msec, TR 80 msec, FA 60°, BW +/-31.25KHz, FOV 16cm, slice thickness 3mm, interslice spacing 0.5mm, 256x256, NEX 4, scan time 1:20).

Figure 8: MRI monitoring allows for detection of faulty injections. The white box on the sagittal scout (left image) shows the location of the time series images. In this canine, the injected contrast/dye solution leaked out of the prostate and into surrounding connective tissue. Therefore, it is known – *during the procedure* – that the desired dose has not been delivered to the prostate.

Figure 9: In both MR images and histological sections, leakage of the injected solution into surrounding tissue is confirmed. Gadolinium-DTPA location (bright enhancement seen in MR images) correlates with blue stained tissue in canine prostate sections. While

some contrast and dye remained within the prostate, additional solution passed into connective tissue at the superior, left, posterior prostate margin.

Figure 10 MRI guidance allows for accurate placement of brachytherapy seeds within the prostate. Three targets were selected in a single coronal plane within the prostate (**row a**) (FSE, TE 9.2 msec, TR 700 msec, BW +/-31.25 KHz, ETL 4, FOV 16cm, slice thickness 3mm, interslice spacing 0.5mm, 256x256, NEX=4, scan time 3:00). The needle was placed at these locations as described previously (**row b**). As the brachytherapy seeds are placed at the end of the canula (2mm back from the end of the trocar tip), the needle artifact is seen to extend beyond the target site by approximately 2 mm. In **row c**, the seeds have been placed within the prostate. The black, bloom artifact at the superior end of the 4 mm brachytherapy seeds is visible. The seeds extend 4mm in the inferior direction from this artifact.

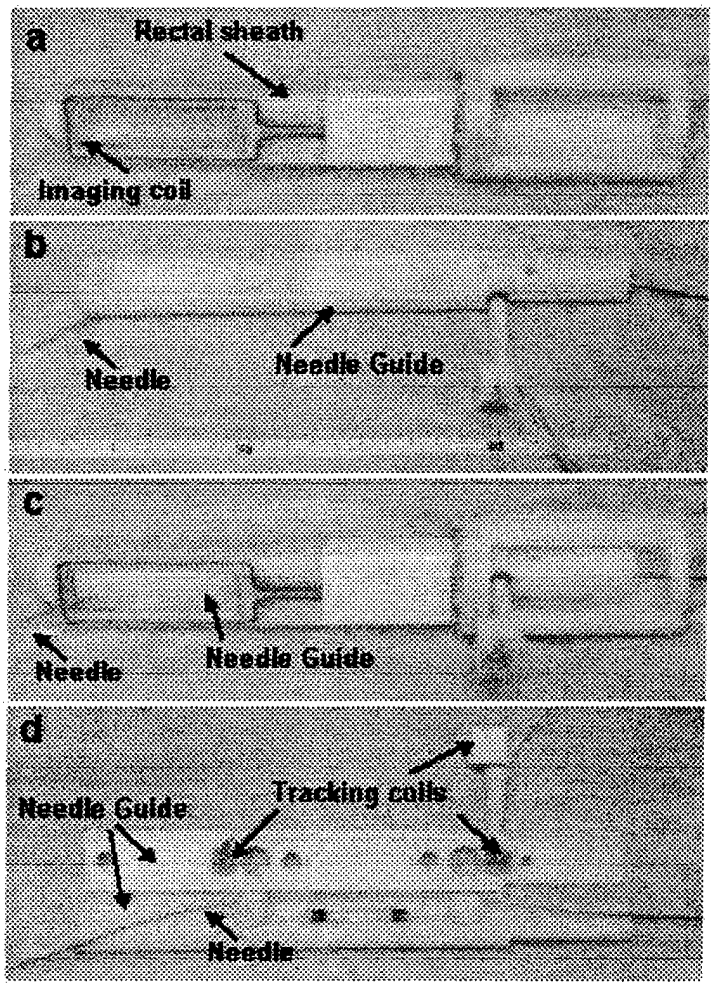

Figure 1: Rectal sheath and needle guide. A stationary rectal sheath, with a radius of 1.5 cm, forms a stable access route through which the prostate can be reached (**Panel a**). A single turn rectal imaging coil, with tuning, matching, and decoupling elements, is included in the sheath. A cylindrical needle guide (**Panel b**) is placed inside of the stationary rectal sheath (**Panel c**), allowing for rotational and translational degrees of freedom. The needle guide includes three tracking microcoils and a curved needle channel, allowing for access to the prostate laterally through the wall of the rectum (**Panel d**).

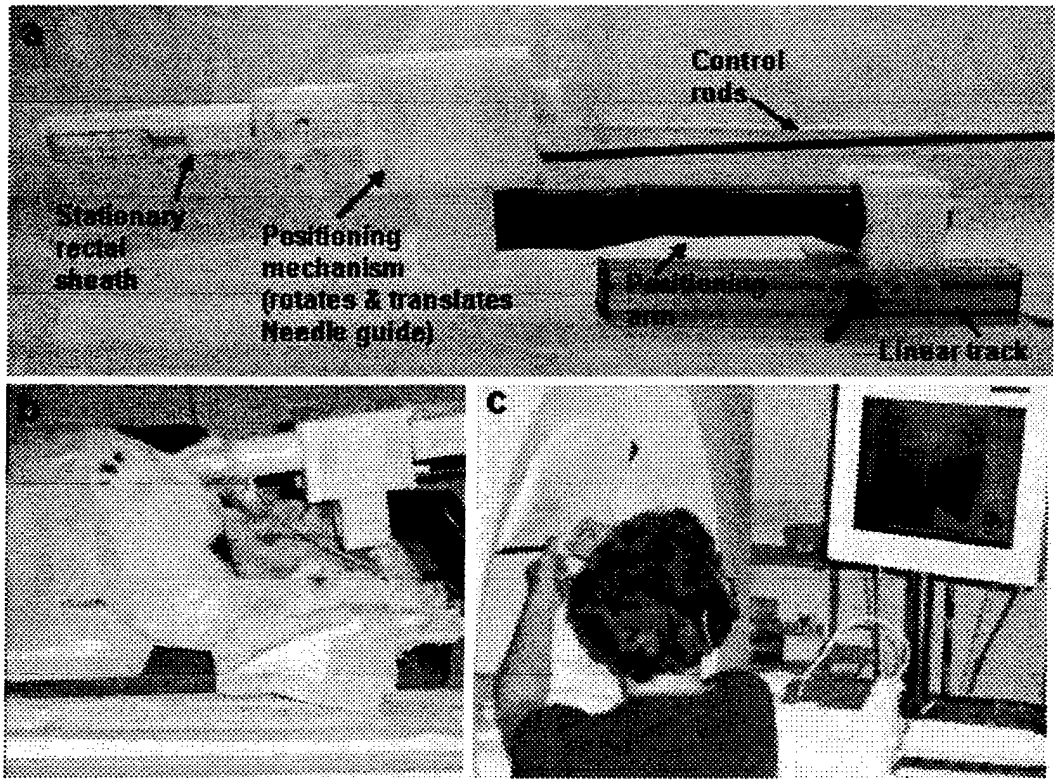

Figure 2: Assembled interventional device. The stationary rectal sheath and needle guide are affixed to the positioning stage (**Panel a**). Via a flexible, articulated arm and a linear track, the device can be positioned freely until both the arm and track are locked into position. The positioning mechanism converts rotation of the two, concentric control rods into rotation and translation of the needle guide within the stationary rectal sheath. The sheath is positioned inside of the subject's rectum and held stationary by the positioning arm and rail (**Panel b**). Via rotation of the two control rods located outside of the bore, the needle guide can be positioned within the rectum (**Panel c**).

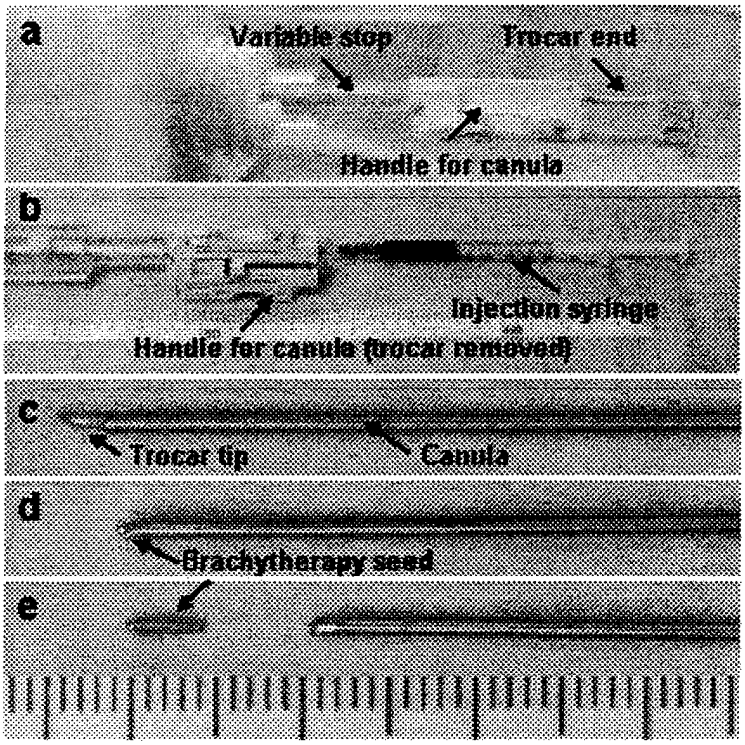

Figure 3: Needle insertion and therapy delivery. A variable stop is used to control the insertion depth of the needle (**Panel a**). After removing the trocar (i.e. the inner stylus), the canula remains as a hollow conduit through which fluid can be injected into the prostate (**Panel b**). To place brachytherapy seeds, the trocar and canula are first advanced together (**Panel c**). Then, after withdrawing the trocar, a brachytherapy seed is pushed to the end of the canula with a second trocar (**Panel d**). Holding the trocar stationary, the canula is withdrawn, ejecting the seed into the tissue (**Panel e**). The trocar and canula are then withdrawn together.

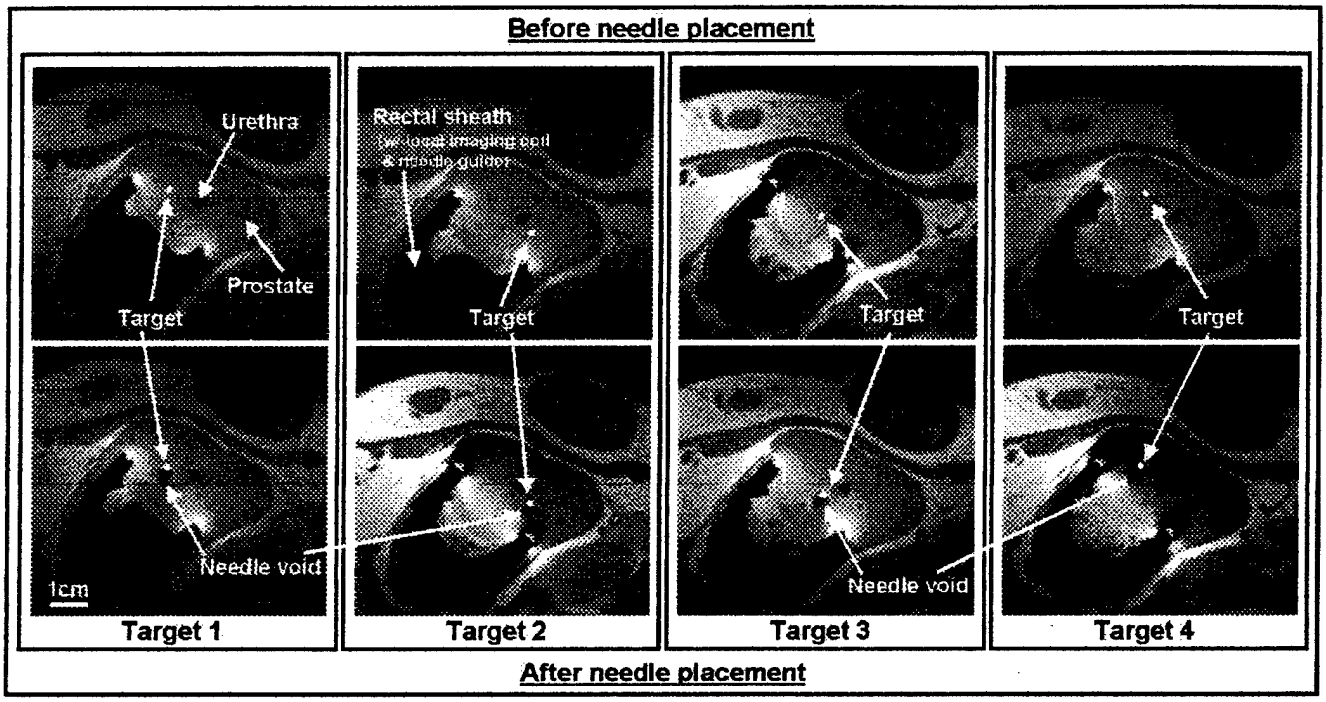

Figure 4: Using the transrectal needle guide and microcoil tracking, needles can be accurately placed within the prostate. In an anesthetized canine, four targets were selected from T1 weighted FSE images (**top row**) (TE 9.2 msec, TR 700 msec, BW +/- 31.25 KHz, ETL 4, FOV 16cm, slice thickness 3mm, interslice spacing 0.5mm, 256x256, NEX=4, scan time 3:00). FSE images were repeated after needle placement (**bottom row**). The needle tip artifact is found in the same slice as the target with an in-plane separation of less than 2 mm. Note also that there is minimal motion of the prostate upon insertion of the needle.

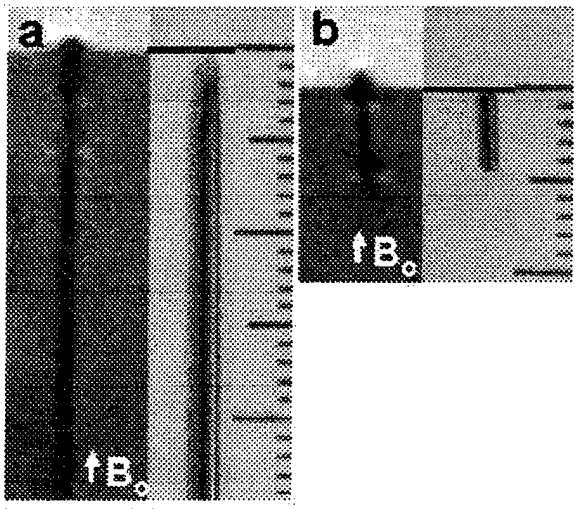

Figure 5: Artifacts created by prostate needle **(Panel a)** and brachytherapy seed **(Panel b)** (FSE, TE 9.2 msec, TR 700 msec, BW +/-31.25KHz, ETL 4, FOV 8 cm, slice thickness 1.5 mm, 256x256, NEX=4, scan time 3:00). Both objects create a uniform signal void along their length and a circular bloom, centered on the object tip, at the end facing the positive pole of the main field. Artifacts were aligned by placing the physical objects at the interface of gadolinium doped and gadolinium free gel blocks.

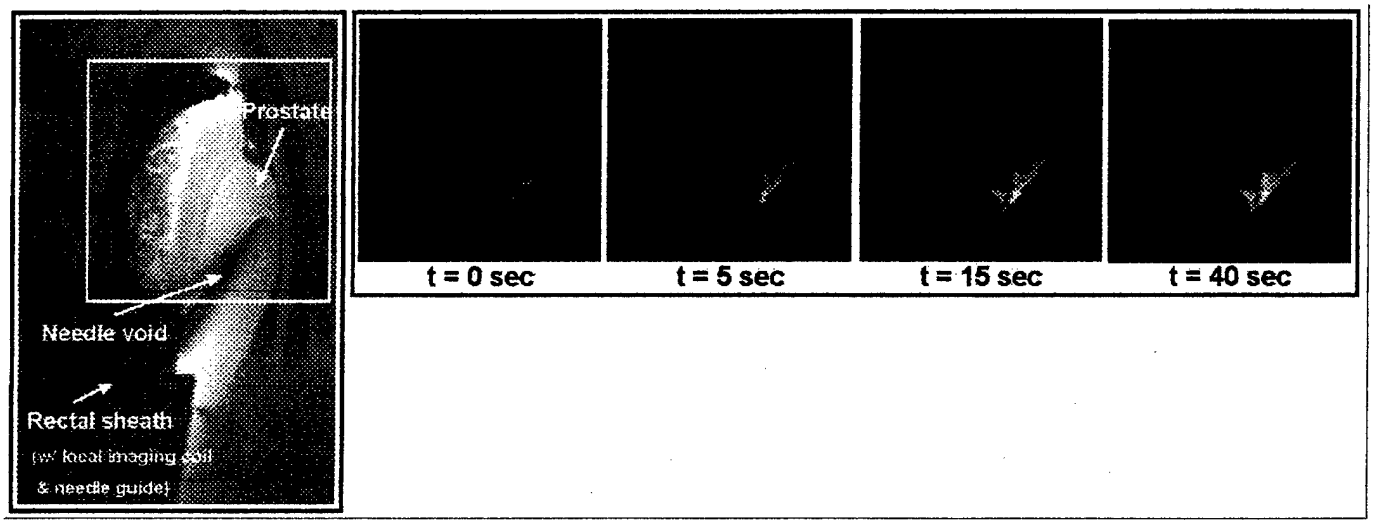

Figure 6: Intraprostatic injections (here, a solution of 0.4% Trypan Blue and 30 mM Gd-DTPA) can be visualized under MRI. The white box on the sagittal scout (left image) shows the location of the time series images. Note that all of the injected contrast/dye solution stays confined within the prostate. Therefore, it was confirmed that the full, desired dose was delivered to the tissue. (FSPGR, TE 1.5 msec, TR 6 msec, FA 90^{o}, BW +/-62.5KHz, FOV 16cm, slice thickness 10mm, 256x160, 0.96 sec/image).

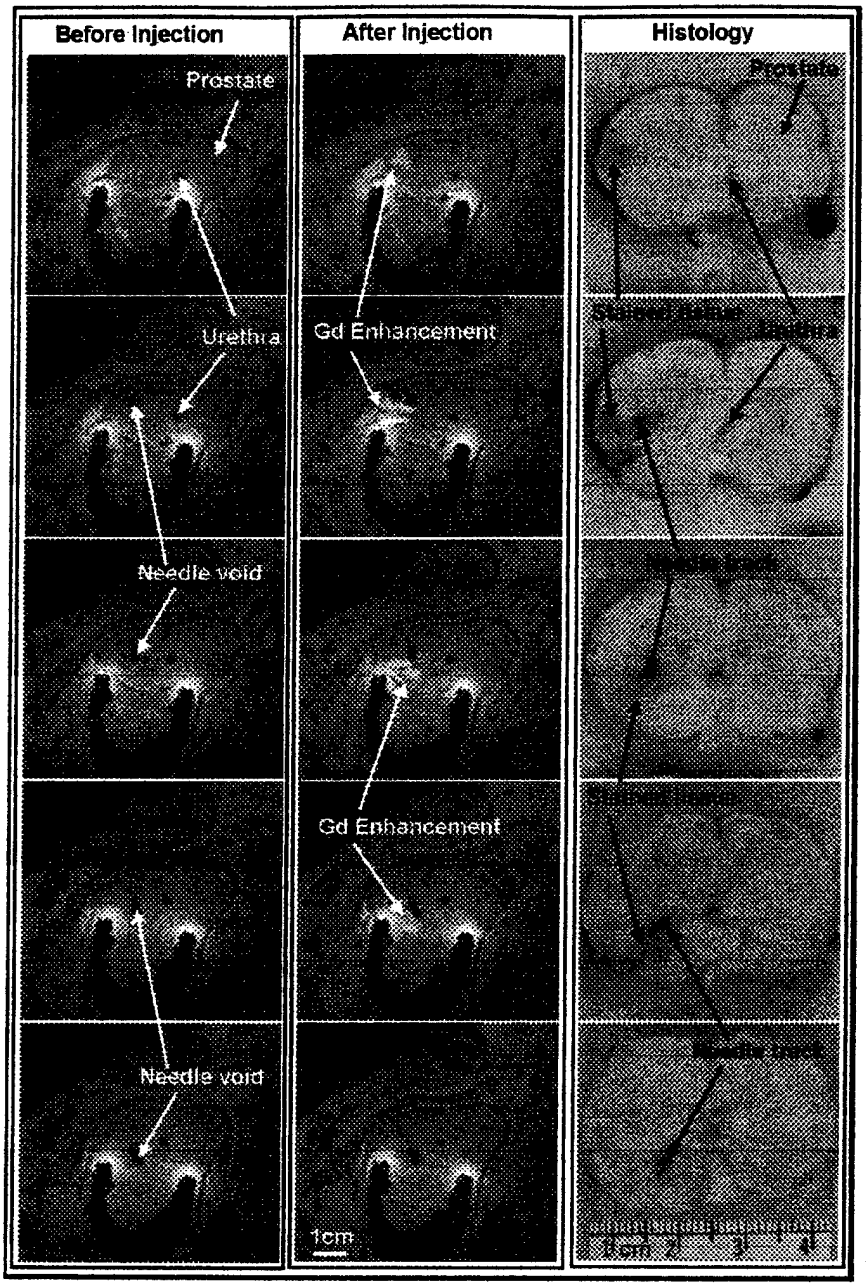

Figure 7: The distribution of injected material visualized in MR images reflects the actual, histologically confirmed distribution. Gadolinium-DTPA location (enhancement seen in post- but not pre-injection images) matches with blue stained tissue in the canine prostate (FSPGR, TE 2.0 msec, TR 80 msec, FA 60°, BW +/-31.25KHz, FOV 16cm, slice thickness 3mm, interslice spacing 0.5mm, 256x256, NEX 4, scan time 1:20).

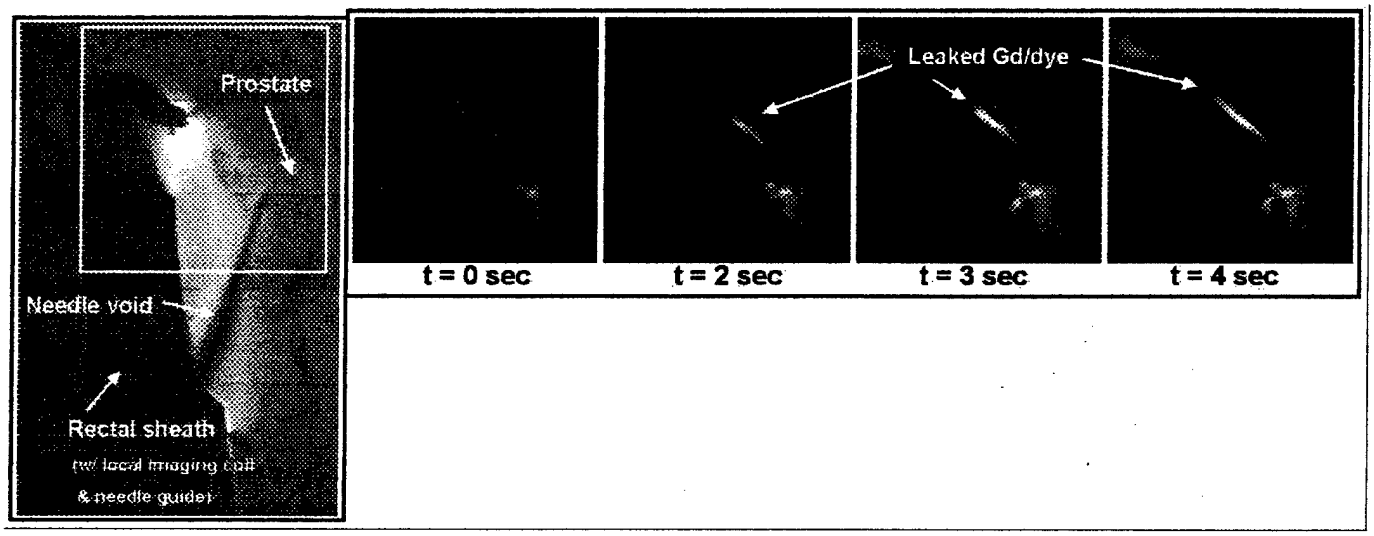

Figure 8: MRI monitoring allows for detection of faulty injections. The white box on the sagittal scout (left image) shows the location of the time series images. In this canine, the injected contrast/dye solution leaked out of the prostate and into surrounding connective tissue. Therefore, it is known – *during the procedure* – that the desired dose has not been delivered to the prostate.

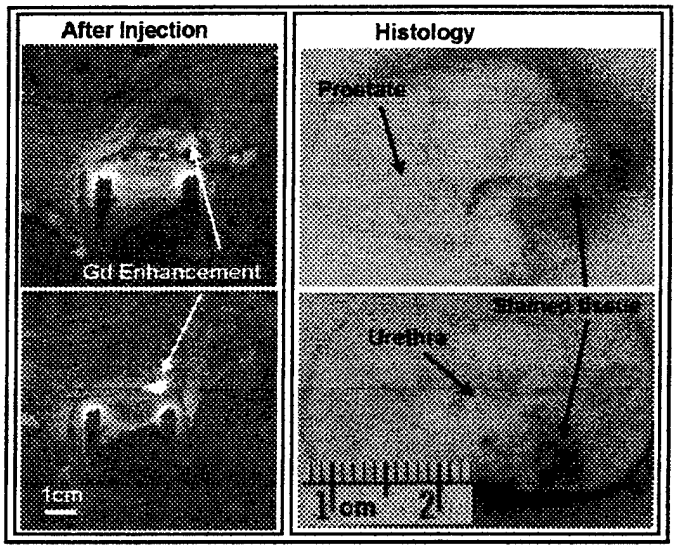

Figure 9: In both MR images and histological sections, leakage of the injected solution into surrounding tissue is confirmed. Gadolinium-DTPA location (bright enhancement seen in MR images) correlates with blue stained tissue in canine prostate sections. While some contrast and dye remained within the prostate, additional solution passed into connective tissue at the superior, left, posterior prostate margin.

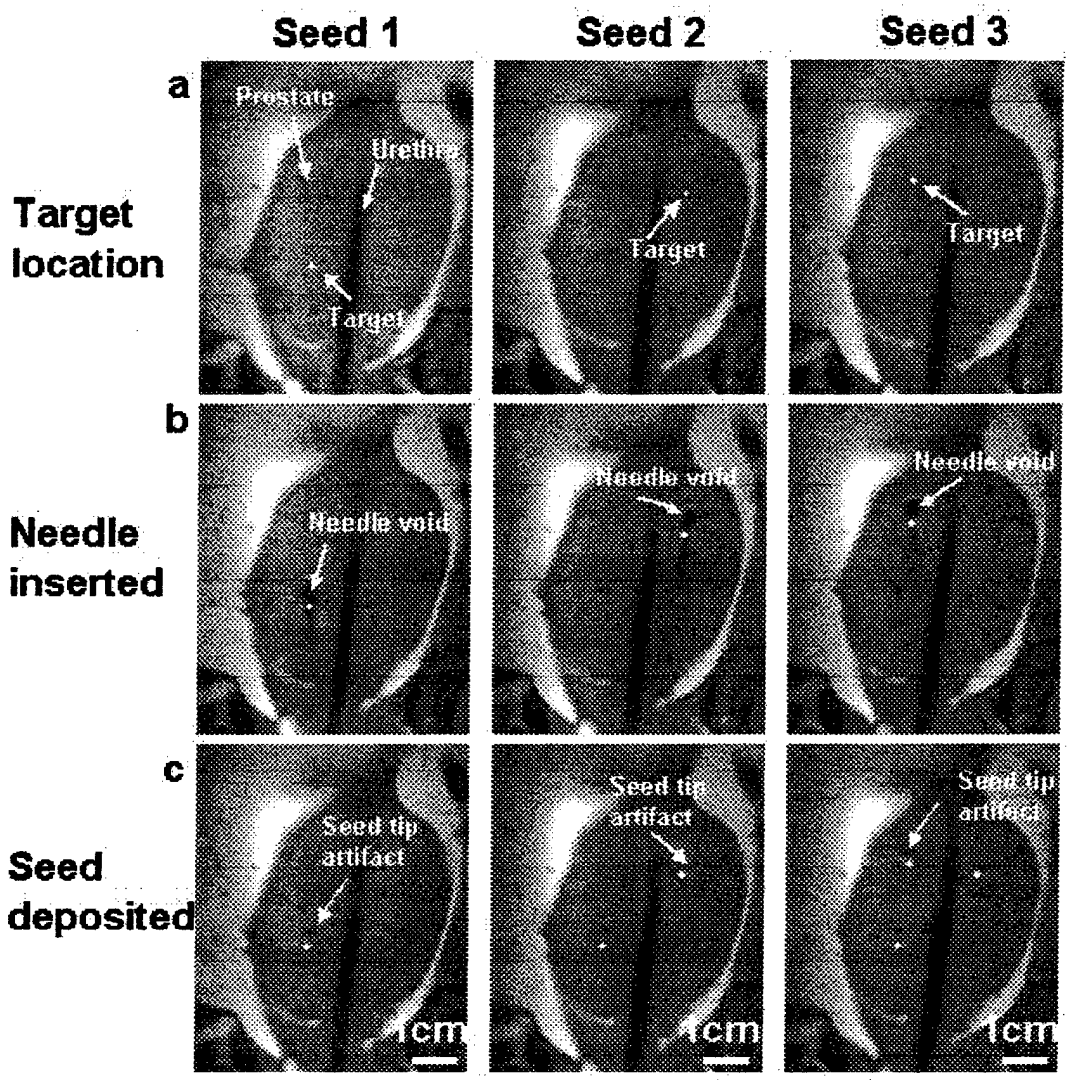

Figure 10 MRI guidance allows for accurate placement of brachytherapy seeds within the prostate. Three targets were selected in a single coronal plane within the prostate (**row a**) (FSE, TE 9.2 msec, TR 700 msec, BW +/-31.25 KHz, ETL 4, FOV 16cm, slice thickness 3mm, interslice spacing 0.5mm, 256x256, NEX=4, scan time 3:00). The needle was placed at these locations as described previously (**row b**). As the brachytherapy seeds are placed at the end of the canula (2mm back from the end of the trocar tip), the needle artifact is seen to extend beyond the target site by approx. 2 mm. In **row c**, the seeds have been placed within the prostate. The black, bloom artifact at the superior end of the 4 mm brachytherapy seeds is visible. The seeds extend 4mm in the inferior direction from this artifact.